NASA TECHNICAL MEMORANDUM

NASA TM X-68200

NASA TM X-68200

APPLICATION OF AN ELECTRONIC IMAGE ANALYZER TO DIMENSIONAL MEASUREMENTS FROM NEUTRON RADIOGRAPHS

by Alex Vary and Kenneth J. Bowles
Lewis Research Center
Cleveland, Ohio 44135

TECHNICAL PAPER proposed for presentation at
Spring Meeting of the American Society for Nondestructive Testing
Los Angeles, California, March 12-15, 1973

APPLICATION OF AN ELECTRONIC IMAGE ANALYZER TO DIMENSIONAL MEASUREMENTS FROM NEUTRON RADIOGRAPHS

by

A. Vary and K. J. Bowles

Lewis Research Center
Cleveland, Ohio

ABSTRACT

Means of obtaining improved dimensional measurements from neutron radiographs of nuclear fuel elements are discussed. This report describes the use of video-electronic image analysis relative to edge definition in radiographic images. Based on this study, an edge definition criterion is proposed for overcoming image unsharpness effects in taking accurate diametral measurements from radiographs. An electronic density slicing method for automatic edge definition is described. Results of measurements made with video micrometry are compared with scanning microdensitometer and micrometric physical measurements. An image quality indicator for estimating photographic and geometric unsharpness is described.

INTRODUCTION

This paper deals with the problems associated with taking measurements from neutron radiographs of nuclear fuel elements primarily to detect dimensional changes from fuel swelling and distortion. It describes an extension of our work reported in reference 1. Previous experience with conventional measurement techniques such as scanning microdensitometry indicated that serious discrepancies in these measurements can occur because of image unsharpness effects (references 2 to 5). A more promising technique for quantitative as well as qualitative analysis of neutron radiographs appeared to be provided by video imaging with electronic enhancement. Therefore, a closed-circuit video-based electronic system was investigated for enhancing and analyzing radiographic images. The purpose of this study was to develop more accurate methods for measuring dimensions from these images. The initial results of this study (reported in reference 1) demonstrated the feasibility of the approach. Therefore, the study was extended and the current paper reports the more recent results and gains in measurement accuracy that were achieved.

The specific goals of the extended study were: (1) to analyze the characteristics of densitometric traces relative to actual superimposed radiographic images; (2) to devise practical empirical criteria for securing accurate dimensional measurements from neutron radiographs; (3) to apply and evaluate electronic image enhancement techniques for edge definition given the unsharpness inherent in neutron radiographs; and (4) to determine the accuracy of these video-based measurements by application to test standards and actual fuel element radiographs. To help achieve these goals, several new

concepts were incorporated into the video system described in reference 1. These added features included video micrometry, video densitometry, and density slicing. The improved image enhancement and measurement capabilities resulting from these additions are featured in this report.

REVIEW OF PROBLEMS AND BACKGROUND

Neutron radiography is increasingly cited as the principle tool for examination of nuclear fuel irradiation effects (references 2 and 6). The fission process in nuclear fuels can cause considerable distortion and swelling of the fuel and its containment cladding. To evaluate these effects, experimental fuel capsules are subjected to irradiation in a high flux reactor and are periodically removed to be neutron radiographed. Because the capsules must not be disassembled, detection of changes due to swelling depends on precise measurements by means of these radiographs. Applicable measurements include: fuel pin diameter, fuel pin length, central void diameter, clad-to-can gap, and cladding thickness.

Most commonly, cylindrical fuel specimens are radiographed perpendicularly to the axis for the purpose of making diametral measurements. A number of factors contribute to uncertainty in making these measurements from neutron radiographs. Included among these factors are: photographic (emulsion) unsharpness, geometric (penumbral) unsharpness, neutron beam and spectrum nonuniformities, variations in film exposure and contrast, and specimen attenuation changes consequent to irradiation (references 3, 4, and 7). All of these factors contribute to the problem of selecting defined "edges" upon which measurements may be based.

Several methods have been used previously for taking measurements from neutron radiographic transparencies: direct viewing, photo-enlargement, optical projection, use of optical comparators, use of traveling microscopes, and use of scanning microdensitometers. With all but the last-named method, the definition of the edge is entirely subjective (i.e., dependent upon the operator's judgment on the location of an edge in the radiograph). However, the scanning microdensitometer yields objective information in that it produces a plot of density variations from which it is possible to "define" the diameter of a cylindrical object. Nevertheless, scanning microdensitometer measurements, although internally consistent, have often failed to give reliable measurements (references 4 and 5).

This paper considers the use of a technique that combines most of the advantages of the previously-mentioned methods of measurements. The image is scanned with a video camera, electronically processed, and displayed on a closed-circuit television screen. This video-based method affords the benefits of direct viewing, magnification, enhancement, micrometry, and densitometry. In addition, edge definition should prove easier to accomplish because more information about the image can be simultaneously displayed on the viewing screen (e.g., superposition of a density scan on the actual

image). This type of video system has, however, not been previously available. Thus, it required study to demonstrate its capabilities for quantitative measurements of radiographs.

The actual fuel elements that were used in this study consisted of uranium nitride pellets clad in the tantalum alloy T-111 (Ta-8W-2Hf). Some of the cylindrical fuel pellets contained voids in the form of axial holes to accommodate swelling and deformation. There was an annular gap separating the cladding from an outer container that consisted of a stainless steel-clad columbium cylinder. In part, this gap allowed for fuel swelling and it contained a helium atmosphere for efficient heat transfer during in-pile tests. Other specimens used in this study were test standards devised specifically to evaluate methods for taking measurements from neutron radiographs of these specimens. The test standards consisted of T-111 cylinders enclosed in an outer cylinder of stainless steel to simulate actual fuel capsules with the exception that these standards contained no fuel. One question that we investigated was whether successful application of video measurements to these standards lead to correspondingly reliable results when applied to actual fuel elements.

APPARATUS

General System Description

The video image analyzer used for this study consists of a closed-circuit television system that includes: (1) a vidicon camera and film illuminator for image acquisition; (2) units for image analysis; (3) and television monitors for image display (see figure 1). The commercially obtained system was originally devised for image enhancement by means of edge enhancement and pseudocolor enhancement methods, references 1 and 8. This system was subsequently modified to include features that permitted analysis and quantitative measurements of neutron radiographic images by video densitometry, video micrometry, and density slicing.

A block diagram of the system is presented in figure 2. For radiographs, a high intensity light source back-illuminates the radiographic film transparencies. The vidicon camera converts the radiographic image to a video signal that may follow one of the several paths indicated in figure 2. For example, the signal may pass through the normal video amplifiers to the monitors for simply viewing the radiograph at various magnifications. By use of different lenses with the vidicon camera, a wide range of magnifications are possible but a practical limit for most radiographs is about 30X. The video signal can also be routed through the edge enhancer for the detection of edge images in radiographs. The results of edge enhancement are discussed in detail in reference 1, and an example is given later in this report.

Another alternative is to bypass the edge enhancer and route the video signal through the density slicer and color generator. The result that will appear on the color monitor consists of a derivative image in which colors

have been electronically substituted for different shades of grey (i.e., light transmission levels) in the original black and white radiograph. There are provisions for inserting up to twelve colors into the displayed image. These colors can be inserted into any portion of the optical density range present in the radiograph. Moreover, each color in the display is controlled by a separate switch so that it can be replaced with black or with the original greytone that it represents. Examples of this type of operation are also given in this report.

The video signal can also be routed simultaneously through the density profiler and normal video amplifiers to perform "video density tracing". The density profiler takes one point on each raster scan line and converts it to a signal that is proportional to the optical density of the radiograph at that point. The output of the profiler appears on the monitors as a density trace along a line on the image (i.e., a plot of light density versus position on the radiograph). This trace is registered with and superimposed on the image itself.

A cursor-generator constitutes the basis of the video micrometer for measuring small dimensions on the radiograph. Two electronically-generated cursors (i.e., white marker lines) are superimposed on the displayed image and are manually aligned with appropriate image elements (e.g., edges) to get linear measurements. Once the spacing between the cursors is calibrated relative to the power of image magnification, the measurement can be read directly in appropriate units from a digital meter.

Video Density Tracing

As in the case of a scanning microdensitometer, the video densitometer yields a trace corresponding to the light transmission of the film as a function of position on the film. The typical shape of a density trace made by scanning across a neutron radiograph of a solid cylindrical specimen is shown in figure 3(a). The distance along the base of this trace may be taken to correspond approximately to the diameter of the cylinder. The white line crossing the image serves to indicate the cross-section along which the displayed density trace is taken. This same line also serves as the base line of the trace. By using a photographic density calibration film strip, the base line can be calibrated to correspond to some preselected density value. Then, density values greater than the baseline value are analyzed and displayed as a function of position on the monitor. The actual density values at various points along the trace can then be read by using the electronically-generated dot reference grid.

Figure 3(b) shows a density trace typical of a cylindrical tube. In this case, the trace is seen to consist of the sum of two curves: a positive curve corresponding to a solid cylinder, and a negative curve corresponding to a cylindrical hole. The distance between the points of intersection of the two component curves can be taken as an approximate measure of the inside diameter of the tube.

It is usual in the case of actual nuclear fuel-pin test capsules to have a number of cylindrical objects fitted together coaxially. Typical neutron radiographs of different parts along the axis of a test capsule appear in figure 4. It is apparent that the resultant density traces consist of portions of a number of curves each representing one of the coaxial cylindrical objects that comprise the fuel element. Another complexity can arise due to the presence of extraneous objects such as thermocouple leads that run axially along the outer surface of the fuel element, e.g., the central peak in figure 4(b). Often, the orientation of the part during radiography results in interference by these extraneous articles with the location and definition of surfaces to be measured. Obviously it is quite difficult to select a suitable approach for making accurate measurements in these circumstances.

Of course, one can make approximate or relative measurements using points of intersection of component curves with each other or with an assumed base line. Alternatively, one can use points of inflection along the slopes of these curves. However, it will be shown that the component curves do not combine to form the composite traces in a simple additive manner. Unsharpness effects in the radiographs tend to modify the resultant traces so that well defined points of intersection are not obvious. It will become evident in this paper that points of inflection or maximum slope are better suited for obtaining accurate measurements.

Video Density Slicing

Reference 1 describes a method for locating edges in radiographic images by an edge enhancement process. The result of the process is illustrated in figure 5 with the neutron radiograph of an experimental fuel capsule. Figure 5(b) is a derivative image which was created by generating a video signal whose amplitude varied proportionally with the rate of change of density along each raster line. The objective of the edge enhancement process is to detect points and linear features that are only faintly registered in the original film image. In accomplishing this, however, it is possible to lose definition of an edge. That is, the edge may be substantially widened in the enhanced image. Nevertheless, edge enhancement can be used as an aid in taking measurements from film images in special cases (reference 1).

Pseudocolor image enhancement is another means of edge definition. Results of this process are illustrated in figures 5(c) and (d). A different color is assigned to each of a number of bands of greytone in a black and white radiograph to clearly delineate density differences. (Figures 5(c) and 5(d) are, of course, black and white reproductions of original color photographs taken from the color television monitor.) This process can be further aided by video density slicing. To illustrate this process all colors save two were switched out of the displayed image for figure 5(d). The lighter of the two remaining colors corresponds to the density slice (i.e., isodensity level) associated with the various edges around

the perimeter of the capsule. It is evident that one can by means of density slicing derive a simplified analog image. This new image can then be more conveniently handled for making measurements.

The relation between the pseudocolor image and video density tracing is illustrated in figure 6. Figure 6 involves the same radiograph as that shown in figure 4(c). The various greytones in figure 6(a) correspond to the following sequence of colors: medium green, dark green, yellow, brown, light red, dark red, and magneta, where medium green corresponds to the peak of the density trace and magenta to the slope portion nearest the black background. Now, in figure 6(b) all colors save light red are switched off and the display consists of only the density slice indicated by the dotted line across the trace.

MEASURING TECHNIQUES

Edge Definition Criteria

The authors of reference 4 proposed a criterion for mathematically relating the shape and dimensions of a microdensitometer trace to the actual diameter of a cylindrical solid. Their method involves the use of transmission values at three different locations on the trace: the maximum value (T_{max}); the background (T_{bg}); and an intermediate criterion value to be used for measurement (T_c). Two of these values (T_{max} and T_{bg}) can be read from the densitometer trace. The third value (T_c) is calculated from $T_c = T_{bg} + \frac{1}{7}(T_{max} - T_{bg})$. Since the video system displays density (D) rather than transmission values and $D = \log \frac{1}{T}$, the equivalent expression for a criterion value for density (D_c) is given by:

$$D_c = -\log \left[10^{-D_{bg}} + \frac{1}{7}(10^{-D_{min}} - 10^{-D_{bg}})\right]$$

(Note: D_{min} corresponds to T_{max})

If D_c is located on the density trace (figure 7) and the distance along the abscissa is measured between the two points corresponding to this density, then the measurement can be related to the actual specimen diameter by a scale factor and a factor that corrects for variations in neutron absorbtion cross sections.

Typically the density range involved in traces examined in this study extended from 2 to 0. Calculated values for D_c for four density ranges of interest appear in Table I.

TABLE I - CRITERION DENSITY VALUES

Background Density, D_{bg}	Minimum Density, D_{min}	Density Difference, ΔD	Criterion Density, D_c	Percent Above Background
1	0	1	0.641	36
2	1	1	1.641	36
2	0.5	1.5	1.247	48
2	0	2	0.820	59

The last column indicates the percent of density range, ΔD, that each D_c value represents. For the range from 2 to 0.5, for example, D_c is found at a point approximately 50 percent of the distance between D_{bg} and D_{min}. (Note that all density traces herein are inverted so that smaller values are above the baseline).

Since the authors of reference 4 found that their "$\frac{1}{7}$" criterion provided a good practical approach to measurement, it was adopted herein to further refine the density slicing procedure as follows. The density trace of a solid cylinder radiograph is assigned seven pseudocolors as indicated in figure 8. Thus, the background density, D_{bg}, is assigned color C_1 and D_{min} is assigned color C_7. Note that each color, C_1 through C_7, represents an equal density slice. For the density range from 2 to 0.5 the operation required by the criterion is accomplished by switching off all but color C_4 (i.e., the 50 percent level). The cylinder would then be outlined as in figure 5(d) or 6(b) on the television display. If the number of colors are doubled for the same density range, then a finer edge definition based on this criterion is possible.

The previously described procedure is subject to errors because neutron radiographic exposures are frequently nonuniform across the region where measurements are made. The effect of this lack of symmetry is further illustrated in figure 9. The ends of the electronically-generated mark are set to coincide with the fuel pin cladding. In figure 9(b) five colors were compressed into the edge region indicated by the ends of the mark. Alternative colors were switched off so that each band of remaining color stands out. The width and spacing of the remaining bands indicate the density gradient near each edge. Clearly, the density gradient on the left is greater than that on the right end of the mark. However the density slicing method of edge definition depends on equal gradients or symmetrical slopes. Therefore, any radiographic exposure can yield poor measurements unless care is taken to assure more uniform neutron flux over the region of interest. This can be accomplished by better collimator designs and by locating items to be measured in positions where the flux profile is flattest.

Although the previously described criterion may suffice for solid cylindrical specimens, it requires modification for cylindrical tubes as in the case of the concentric cylinders shown in figure 10. Here, none of the component curves is complete, and therefore ΔD and D_{min} must be inferred. Since the intersections of the curves are fairly well defined, one can use them to estimate diameters. Thus, to estimate the outside diameter the cursors can be set to match the intersection of the outer curve with the background as indicated in figure 10(a). To estimate the inside diameter, the cursors would be matched as in figure 10(b). The outside and inside diameters of the annular gap are estimated as indicated in figures 10(c) and 10(d), respectively.

It is instructive to examine the density trace in the gap region closely. Figure 11(a) shows how the densitometric trace might appear without any unsharpness effects in the radiograph. The actual appearance of the trace invariably resembles figure 11(b). This is apparent in the radiograph shown in figure 12(a) and especially in the magnified views of figures 12(b) and (c). Therefore, some method for estimating the value of the unsharpness, U, is required if it is planned to take measurements as indicated in figure 10. To arrive at a practical method, first consider the manner in which unsharpness curves interact. In figure 13, each of the two edges of the slit depicted in an end view will independently register a radiographic image having an "S"-shaped density trace, as indicated. These "S"-shaped unsharpness curves interact to yield a resultant trace having the form shown by the solid line (reference 9). As the slit widens, the height of the trace will reach a maximum for a particular width. This width, w_{max}, depends on the radiographic exposure conditions and particularly on relative distances between the slit, radiographic film, and neutron source, given a fixed slit material and thickness. One-half w_{max} can be taken as an estimate of unsharpness, U, because for w-values greater than w_{max} no further unsharpness interaction occurs and because each edge contributes only half of the total unsharpness of the whole slit.

A density trace similar to that associated with the radiograph of a series of slits is shown in figure 14(a). In this case, the radiograph is of a neutron radiographic test object (or image quality indicator, IQI) consisting of cadmium foil. The foil is 25.4 microns (1 mil) thick and contains a series of hexagonal holes. Each of the seven webs separating the holes is a different size ranging from 28 microns (1.1 mils) to 165 microns (6.5 mils) in roughly equal steps, e.g., the fourth web indicated by the cursor pair is 96 microns (3.8 mils). Figure 14(b) is a plot of the density amplitude produced by each web against web width normalized relative to D_{min}-D_{bg} in figure 14(a). Extrapolated to unity on the ordinate, the mean intercepts it at an abscissa value of approximately 230 microns (9.0 mils). Thus, for the conditions of this particular exposure, 115 microns (4.5 mils) is the estimate of unsharpness (i.e., w_{max} = 230 microns = 2U, in this case). The unsharpness value for U estimated in this manner will vary according to the distance between the IQI and the neutron radiographic image transfer foil. (See ref. 10 for a description of the neutron radiography procedure.) Placed in direct contact with the foil, the IQI image should

be affected only by photographic unsharpness factors. But, at any distance from the foil, the IQI image will also include the effects of geometric unsharpness factors. Therefore, to estimate the total unsharpness, U, in radiographs, the IQI should be radiographed with and located in the same plane as the edges of the object whose radiographic image will be measured.

The previous discussion forms the basis for obtaining appropriate measurements from fuel element neutron radiographs. By examination and measurement of numerous radiographs of cylindrical solids it was found that the criterion value for D_c invariably occurs at the point of inflection of curvature of the density trace. This is the point of maximum gradient. The relation between edges and partial curves (such as those in the traces of figures 3, 4, and 10) were examined and again noted that the known edges coincided with points of maximum gradient. It appeared, therefore, that even in cases where D_c is not readily calculated, the point of maximum gradient (inflection point) suffices to define the edge. Density slicing can be used to locate these points since they yield the minimum width color slice for one of a series of colors assigned to the edge region (e.g., see figure 9). This provides an objective criterion for edge definition, and as explained later, this particular criterion was tested by application to specially constructed test standards.

In the case of scanning microdensitometry traces it is conventional to use peak-to-peak measurements as illustrated in figure 10, see reference 5. This is a convenient approach because peaks are easy to locate and it suffices if only relative changes (such as swelling) are being measured. As noted previously, however, these peaks will be offset from the actual edge by an amount determined by unsharpness effects. In the next section diameters determined by peak-to-peak measurements will be compared with those determined by video via the inflection point criterion. It will be apparent that the error based on peak-to-peak readings equals that predicted by unsharpness estimated with the previously described IQI.

Test of Edge Definition Criteria

Since the ultimate objective of this work was to measure dimensional changes in nuclear fuel capsules, test standards were constructed with similar materials and dimensions (but without fuel). A neutron radiograph of two of these standards and an IQI for determining unsharpness are shown in figure 15. This neutron radiograph was made at NASA's Plum Brook reactor facility. The larger standard in figure 15 consists of a tantalum alloy cylinder inside a stainless steel cylinder. The outside diameter of the tantalum cylinder has five machined steps. The steps increase in size to simulate fuel clad swelling. The smaller test standard represents a different size fuel capsule and consists of a uniform diameter tantalum cylinder coaxial with a stainless steel cylinder.

In table II are a series of tantalum cylinder measurements that were made using the inflection point criterion with the video system for the two standards described above.

TABLE II - STEPPED STANDARD CLAD DIAMETER MEASUREMENTS

Physical measurements		Video micrometer measurements		
Diameter, mils	Diameter, millimeters	Diameter[a] (average), millimeters	Standard deviation, microns	Percent[b] error
715.1	18.16	18.22	31	0.33
722.6	1835	18.37	41	0.10
729.5	18.53	18.57	43	0.21
736.6	18.71	18.73	31	0.10
743.8	18.89	18.87	23	0.10
373.0[c]	9.474[c]	9.499[c]	51[c]	0.27[c]

a. Ten equally-spaced measurements were made and averaged for each part of the test standards.
b. Percent error is based on column three relative to column two.
c. Measurements for the smaller nonstepped standard (see figure 15).

The tabulation indicates the average value of the series of ten diameter measurements made at equal intervals on each step and compares it with the physical measurement made with a micrometer prior to assembly (see the percentages in the last column). The standard deviation is less than 43 microns (1.7 mil) for all the measurements taken on the larger five-step standard in figure 15. The standard deviation is a measure of the scatter that is indicated in figure 16 for each of the five steps of the standard. A co-plot of diameter measurements made with three methods on the radiograph of the stepped standard appears in figure 16. The triangles show results obtained with a scanning microdensitometer trace involving peak-to-peak measurements. The other data points were obtained with the video system. One set of these points was obtained with edge definition by the inflection point criterion. Another set was obtained purely by eye judgment of edge location on an unenhanced television image at a magnification of approximately 9X. The densitometer peak-to-peak readings consistently exceeded the known physical dimensions by from 217 microns (8.5 mils) to 370 micron (15 mils). These values are comparable to the minimum unsharpness value of 230 microns (9 mils) estimated from the IQI image. This illustrates that the peak criterion commonly used in scanning microdensitometry fails to give accurate measurements for the reasons explained previously in this paper. After working extensively with the video system, it was found that measurements could be made even without the elaborate density slicing procedures described previously. In fact, once the information afforded by density slicing and density tracing was in hand, the cursors could be aligned quite

well by eye. The aids could thus be abandoned once they provided the necessary clues to guide eye judgment. The additional small error introduced may be worth the time-savings gained by use of this simplified method. But even though the remarkable acuity of the human eye is thus verified, there still remains the need to assure automatic methods for edge definition and measurement.

Measurements of Actual Fuel Elements

With these techniques in hand, radiographs of irradiated experimental fuel were then examined with the video system. A radiograph of one of the nine fuel elements evaluated appears in figure 17. The diametral measurements presented here were made after the elements were exposed for 9000 hours in a high flux reactor at the Oak Ridge National Laboratory (ORNL). Since three of these fuel elements were placed in tandem and each was approximately 11 cm (4.5 inch) long, the radiographic exposures were subject to nonuniformities due to axial variations of neutron flux. (The fuel elements were neutron radiographed at the ORNL reactor facility.) Axial density traces were made to check for this factor. Severe gradients in the neutron flux could have affected the diametral measurements made from the radiograph. In this case, however, the small variation of density that was detected in the axial direction was deemed insignificant. Another factor considered was the slight magnification peculiar to the radiographic facility. (This can be calculated from the relative spacing of the specimen, neutron source, and image foil.) The video measurements were corrected for this magnification factor and plotted in figure 17 which indicates a considerable bulge in the fuel element. It is also seen that the video measurements agree with physical measurements made after the elements were removed from their containers. The physical measurements were made at the ORNL hot laboratory with opposing microgauges that had been calibrated on a standard cylinder.

The essential observation to be made is that a relatively small amount of clad swelling (approximately 2.8 percent of the diameter) was detected by means of the video technique. Thus, this technique offers an accurate and reliable means of measuring fuel swelling from radiographs taken at various intervals during a long-term irradiation test sequence. It should be noted that good results were obtained despite factors that tended to obscure edges in the radiographic image. For example, in the case of the actual fuel elements, as the one in figure 17, thermocouple sheaths and other articles were unavoidably superimposed on the fuel element image. These sometimes interfered with the edge definition procedure.

DISCUSSION OF RESULTS

The video-based method of measurement described herein was tested for accuracy and reproducibility. It was recognized that even with the aids for edge definition provided by density traces and slices, judgment was required to accurately align the cursors with the edges. By its nature this procedure can lead to a false indication because of the accumulation of a

number of small errors of judgment. Our method, therefore, involved a deliberate upsetting and resetting of the cursors for each of the series of measurements made along each of the steps in the test standards. This removed the possibility of a constant systematic error but introduced a statistical error. This explains the scatter indicated in figures 16 and 17. Thus, the scatter was fostered by the above-described method of aligning the cursors. This method was adopted because it imposed a burden and thereby provided a gauge of the amount of variation to be expected from the video measurements. The greatest variation was less than $\pm$ 0.5 percent in all the readings made. And, as seen for the cases presented in table II, the total error was always less than~0.3 percent between the video average and physical measurements.

Magnifications best suited to the video measurements were also studied. It should be noted that magnification is no panacea for edge definition or precision of measurement. A magnfication of about 10X and less on the television monitor screen is adequate in most instances. Greater magnifications up to 30X were studied, but the effects of film mottling and graininess became impediments to edge definition (see figures 12(b) and (c) for example).

There should be enough magnification so that a sufficient number of raster scan lines are included in the region of interest. Obviously, the limiting width of a density slice band will be that of a single scan line where the edge is parallel to the raster scan. Typically, it is best to magnify the image only to the extent of filling only the central 80 percent of the monitor screen with the region of interest for measurement. Beyond this distortion prevails. Inside this domain we found the accuracy to be within $\pm$ 0.2 percent for measurements taken over the same distance as the cursor calibration length and within $\pm$ 1 percent for any arbitrary length that differed from the calibration length. These percentages are based on film calibration standards having well-defined linear graduations that were used to calibrate the cursor spacing indicator prior to taking measurements from specimen radiographs.

Generally, it was found that the video-based measurements agreed well with physical measurements. An advantage over scanning microdensitometry was afforded by the video system because with it one can view, manipulate, and enhance the image while defining edges and making measurements. Use of the video system was found to provide a substantial saving in time and effort relative to scanning microdensitometry in taking measurements from typical neutron radiographs. Video measurements are easier to set up and accomplish. Production of a video density trace is instantaneous while the scanning densitometer involves a slow mechanical process. For a given set of measurements the video method can be accomplished about ten times faster than scanning microdensitometry.

Automation of the measurement process is possible with the video system. Density slicing lends itself to automation since it isolates image details that can be more easily recognized and processed by computer techniques.

Moreover, the video system provides a means of dealing in real-time with images such as those produced by X-ray or neutron-sensitive videcons. Thus, it should be recognized that the system described in this paper has potentially wide application to a wide variety of images on which linear measurements are required.

CONCLUSIONS

We concluded that the video system described herein is a reliable and accurate tool for making measurements of nuclear fuel pin dimensions and dimensional changes via neutron radiographs. This conclusion is supported by measurements made with the system and comparisons with scanning microdensitometer and actual physical measurements on test standards and irradiated fuel elements. Perhaps the most important conclusion to be drawn from this investigation is that video-electronic image analysis not only affords reliable and accurate measurements from radiographs, but that it substantially reduces the time and effort required to make these measurements. This was borne out by direct comparisons with other methods of measurements, particularly scanning microdensitometry.

Moreover, we found that this system provided information relative to establishment of criteria for edge definition. This information was based upon a study of electronic superposition of density traces on radiographic images displayed on the television monitor. Our criterion is based on locating the point of inflection or maximum gradient on a density trace.

It was also found that the frequently-used peak-to-peak measurements on densitometric traces yield erroneous values because these peaks do not correspond to actual edges. This is attributable to unsharpness effects in the radiographs. Therefore, we investigated an image quality indicator that proved useful for estimating unsharpness in a radiograph. Unsharpness values estimated by means of the indicator were verified by comparing measurements from densitometric traces and direct physical measurements.

We also found that the system provided a useful means of objective edge definition by means of a color density slicing procedure based on our edge definition criterion. This procedure yields a highly simplified version of the radiograph since it eliminates extraneous details. We concluded that this feature of the system promises to be a significant adjunct to automating the process of making measurements from virtually any type of image.

REFERENCES

1. A. Vary, "Investigation of an Electronic Image Enhancer for Radiographs," Materials Evaluation, Vol. 30, No. 12, Dec. 1972, pp. 259-267.

2. H. Berger, "The Present State of Neutron Radiography and Its Potential," Materials Evaluation, Vol. 30, No. 3, Mar. 1972, pp. 55-65.

3. I. Panaitescu, "Assessing the Quality of a Radiographic Image," Materials Evaluation, Vol. 29, No. 7, July 1971, pp. 153-158, 164.

4. S. J. Basham, D. R. Grieser, and J. W. Ray, "Dimensional Measurements of Cylindrical Specimens Using Neutron Radiography," Materials Evaluation, Vol. 28, No. 6, June 1970, pp. 140-144.

5. L. A. Thaler, "The Measurement of Capsule Heat Transfer Gaps Using Neutron Radiography," NASA TM X-67920, Oct. 1971.

6. A. M. Plummer, "Reactor Materials Inspection by Neutron Radiography," Reactor Technology, Vol. 14, No. 1, Spring 1971, pp. 1-6.

7. B. E. Foster, V. A. Snyder, V. A. DeCarlo, and R. W. McClung, "Development and Operation of a High-Intensity, High-Resolution Neutron Radiography Facility," Oak Ridge National Laboratory Rep. No. 4738, Dec. 1971.

8. R. H. Stratton, and J. J. Sheppard, Jr., "A Photographic Technique for Image Enhancement: Pseudocolor Three-Separation Process," RAND Corp., Rep. No. R-596-PR, Oct. 1970.

9. E. L. Criscuolo, "Slit Detection by Radiography," Materials Evaluation, Vol. 24, No. 4, Apr. 1966, pp. 201-205.

10. H. Berger, Neutron Radiography, Elsevier Publishing Co., N. Y., 1965.

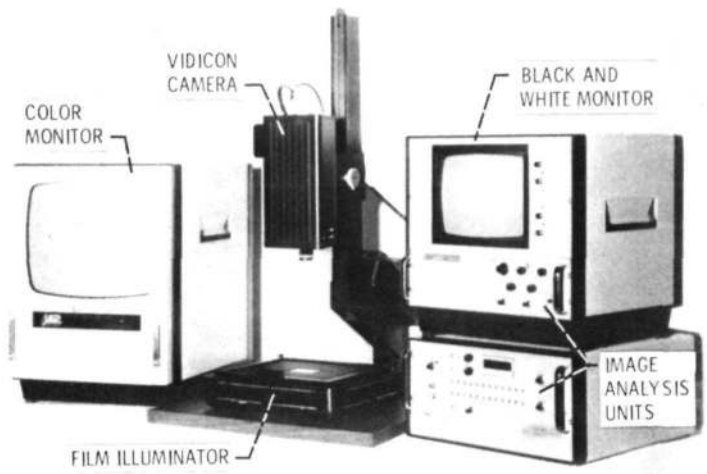

Figure 1. - Electronic image analyzer.

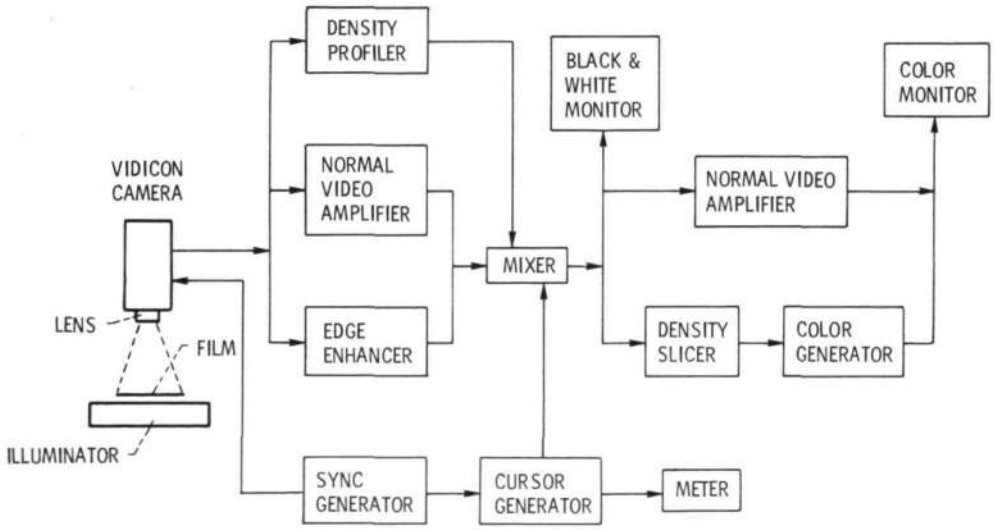

Figure 2. - Image analysis system block diagram.

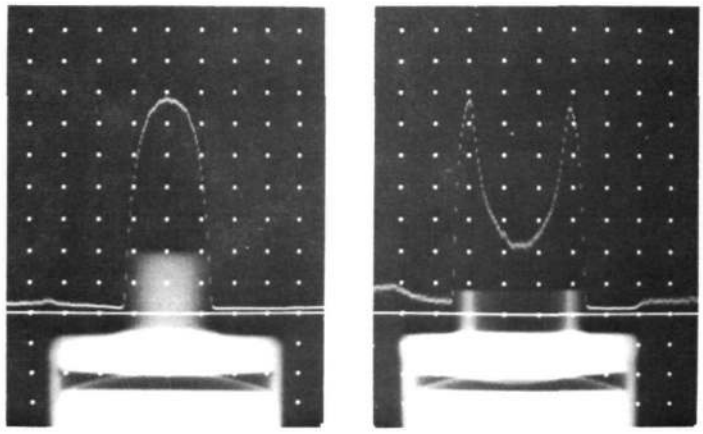

(a) TYPICAL DENSITY TRACE FOR A SOLID CYLINDER.

(b) TYPICAL DENSITY TRACE FOR A CYLINDRICAL TUBE.

Figure 3. - Video density traces on a neutron radiograph of an experimental nuclear fuel capsule.

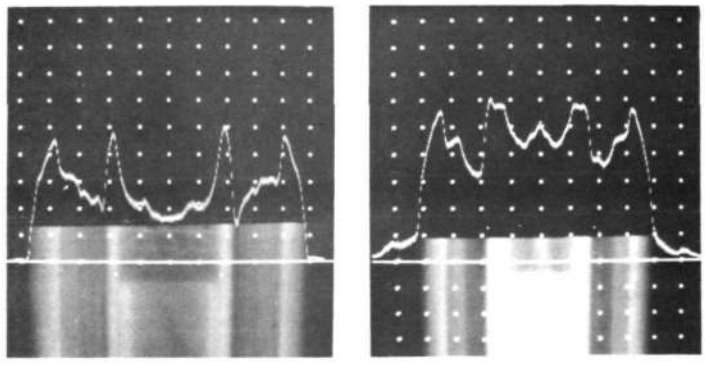

(a) DENSITY TRACE AT UNFUELED END OF FUEL ELEMENT.

(b) DENSITY TRACE IN ZONE NEAR NUCLEAR FUEL PELLET.

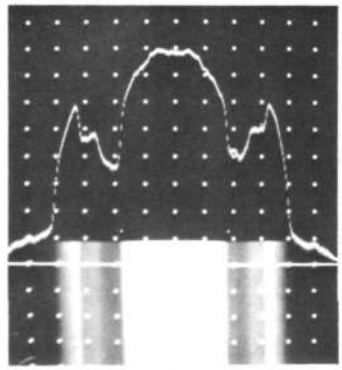

(c) DENSITY TRACE THROUGH NUCLEAR FUEL PELLET.

Figure 4. - Video density traces on a neutron radiograph of a nuclear fuel element enclosed in coaxial cylinders.

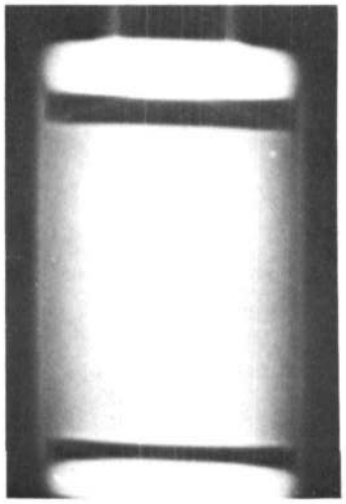

(a) NORMAL RADIOGRAPH.

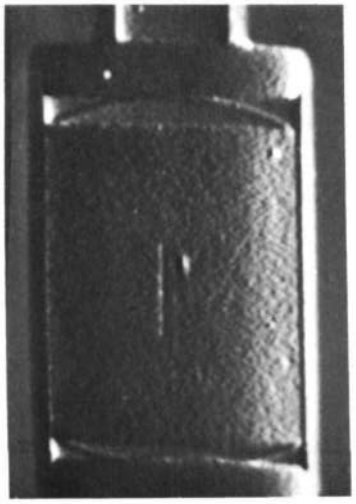

(b) EDGE ENHANCED.

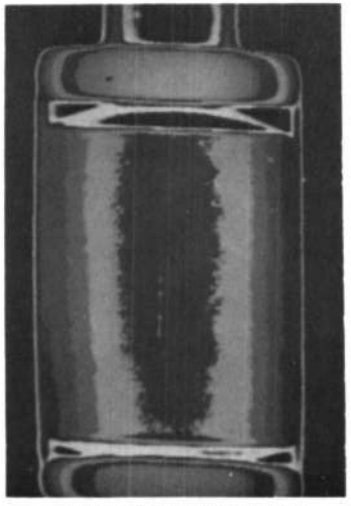

(c) PSEUDOCOLOR ENHANCED.

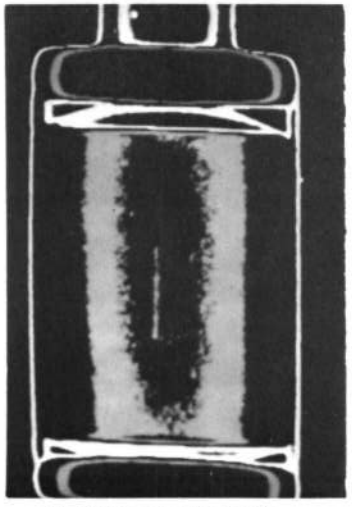

(d) COLOR DENSITY SLICED.

Figure 5. - Electronic enhancements of a neutron radiograph of an experimental nuclear fuel capsule.

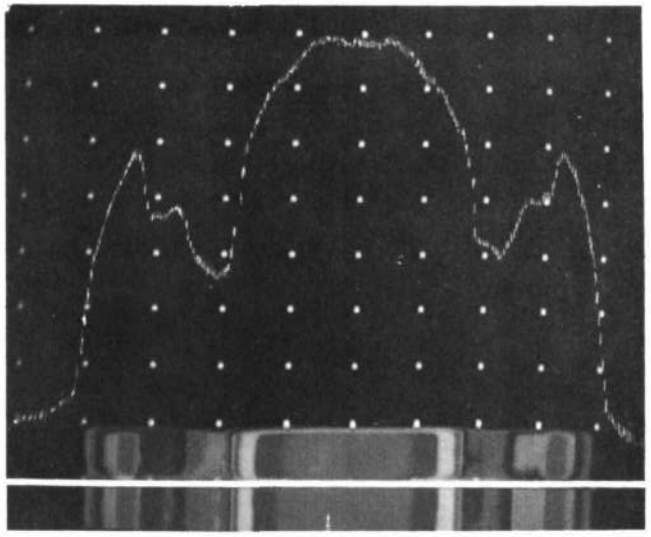

(a) RELATION BETWEEN DENSITY TRACE AND PSEUDOCOLOR IMAGE.

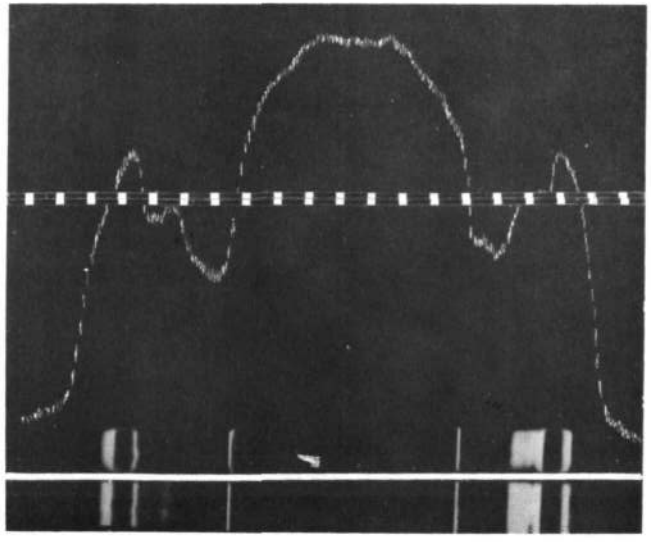

(b) DENSITY SLICED IMAGE AT PRESCRIBED DENSITY LEVEL.

Figure 6. - Pseudocolor enhancements of the neutron radiograph of a nuclear fuel element enclosed in coaxial cylinders.

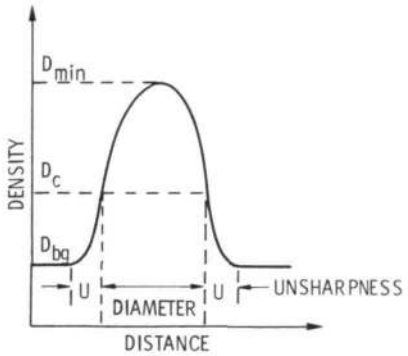

Figure 7. - Typical density trace of a radiograph of a solid cylindrical object indicating relation to its diameter.

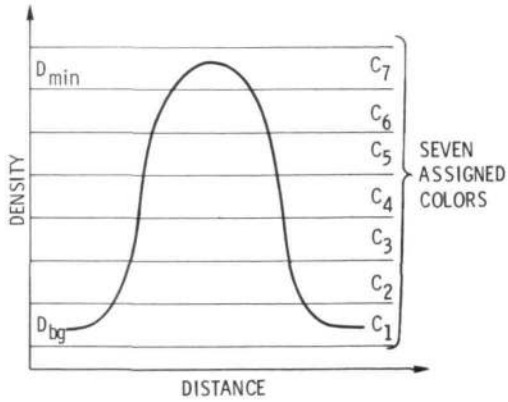

Figure 8. - Typical density trace for a solid cylindrical object and indication of pseudocolor assignment scheme.

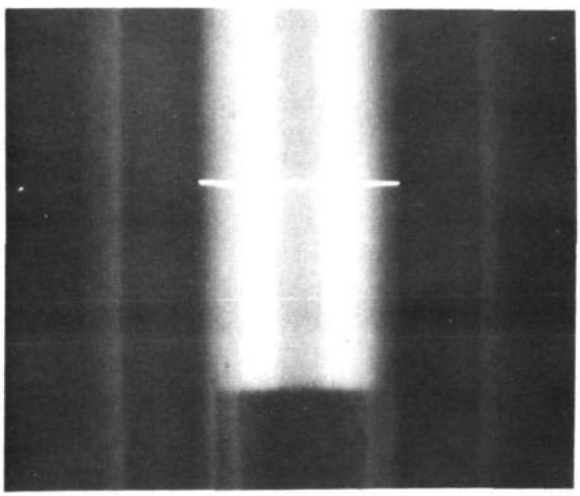

(a) RADIOGRAPH WITH MARKER INDICATING CLADDING OUTSIDE DIAMETER.

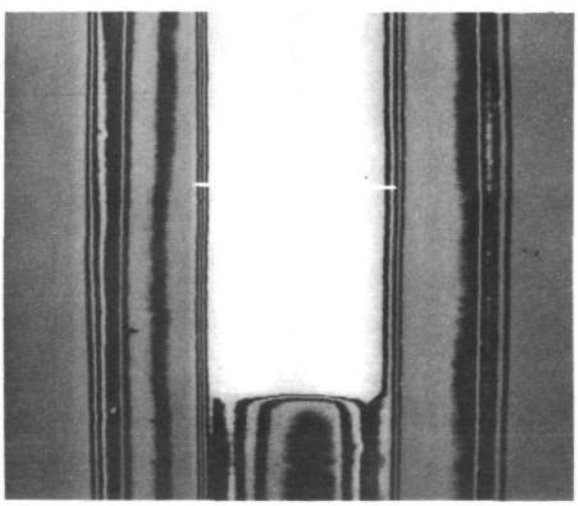

(b) DENSITY-SLICED RADIOGRAPH SHOWING DENSITY GRADIENT VARIATION.

Figure 9. - Enhanced neutron radiograph of a nuclear fuel element exhibiting density gradient difference on opposite sides of fuel cladding.

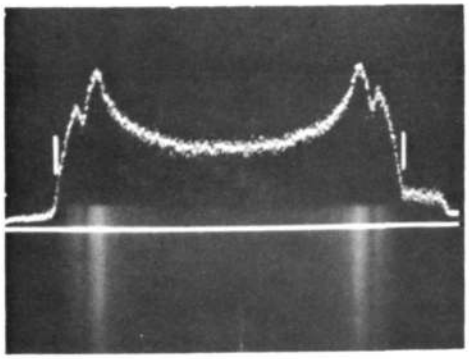

(a) OUTSIDE DIAMETER OF OUTER CYLINDER.

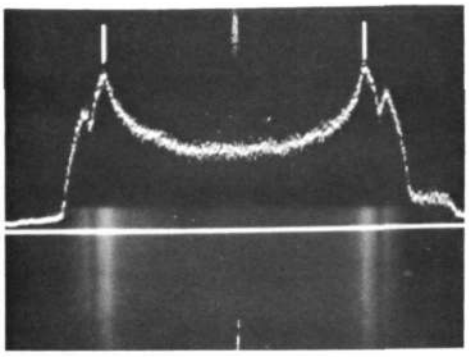

(b) INSIDE DIAMETER OF INNER CYLINDER.

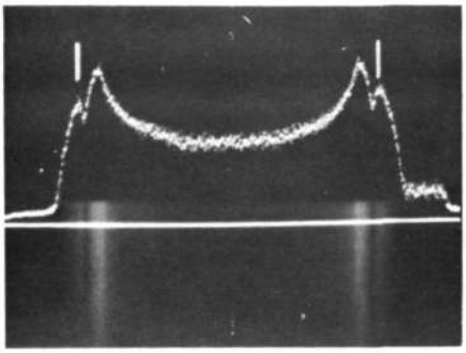

(c) OUTSIDE DIAMETER OF ANNULAR GAP.

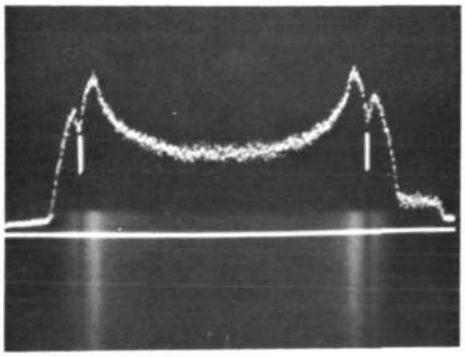

(d) INSIDE DIAMETER OF ANNULAR GAP.

Figure 10. - Density traces illustrating alignments of video micrometer cursors to take approximate measurements from the image of coaxial cylinders separated by an annular gap.

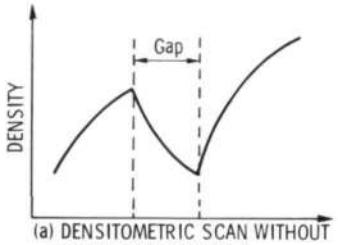

(a) DENSITOMETRIC SCAN WITHOUT UNSHARPNESS EFFECTS.

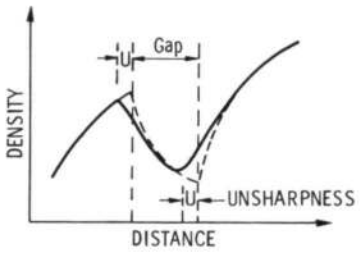

(b) DENSITOMETRIC SCAN WITH UNSHARPNESS EFFECTS.

Figure 11. - Theoretical density traces for the annular gap region of a radiograph of a solid cylinder enclosed concentrically with a cylinder tube.

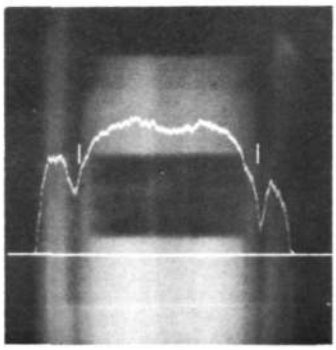

(a) CURSORS MATCHED WITH CLADDING OUTSIDE DIAMETER FOR COMPARISON WITH PEAKS.

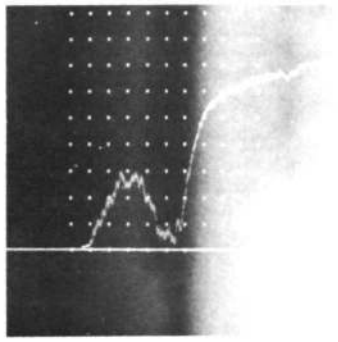

(b) MAGNIFIED IMAGE SHOWING TRACE THROUGH THE LARGER CAN-TO-CLAD GAP.

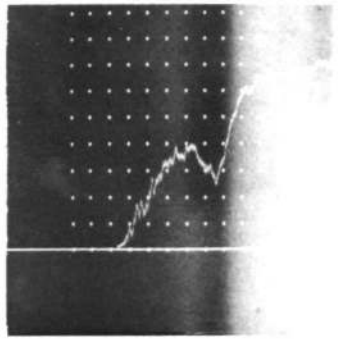

(c) MAGNIFIED IMAGE SHOWING TRACE THROUGH THE SMALLER CAN-TO-CLAD GAP.

Figure 12. - Density traces on a nuclear fuel capsule radiograph showing peak displacement due to unsharpness effects.

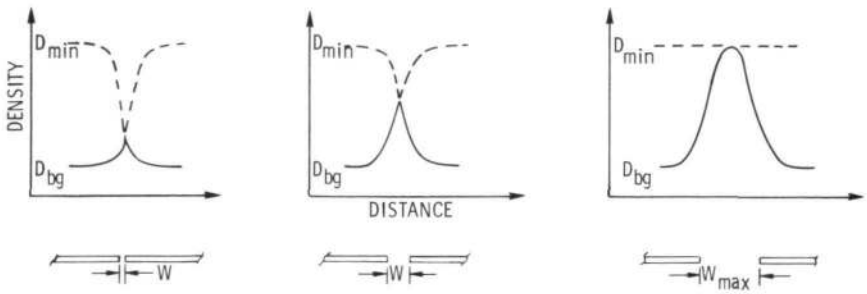

(a) SLIT WIDTH APPROACHING ZERO.

(b) INTERMEDIATE SLIT WIDTH.

(c) SLIT WIDTH OF MAXIMUM TRANSMISSION.

Figure 13. - Theoretical density trace of interaction of unsharpness curves for a radiograph of a slit.

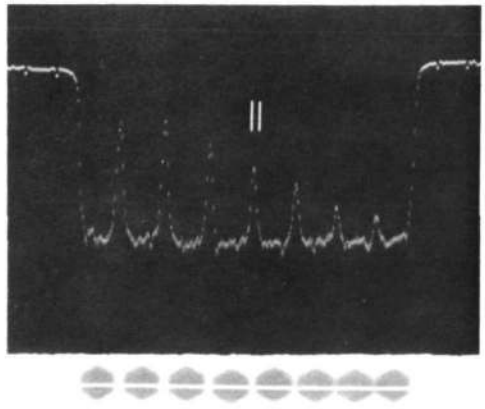

(a) DENSITY TRACE ON IQI NEUTRON RADIOGRAPH.

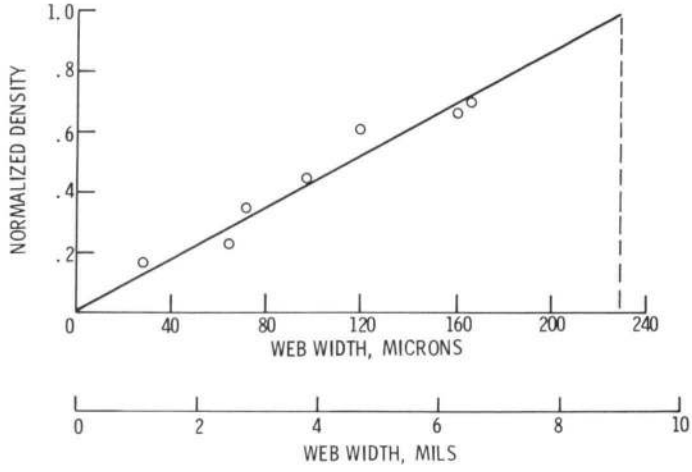

(b) UNSHARPNESS ESTIMATION PLOT.

Figure 14. - Method of estimating unsharpness effects using a neutron radiograph of a cadmium foil image quality indicator (IQI).

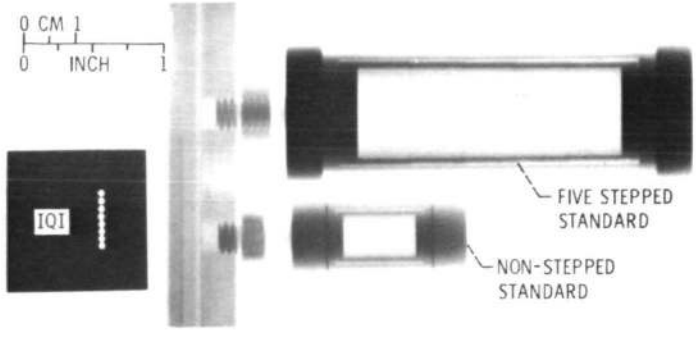

Figure 15. - Neutron radiograph of simulated fuel element test standards.

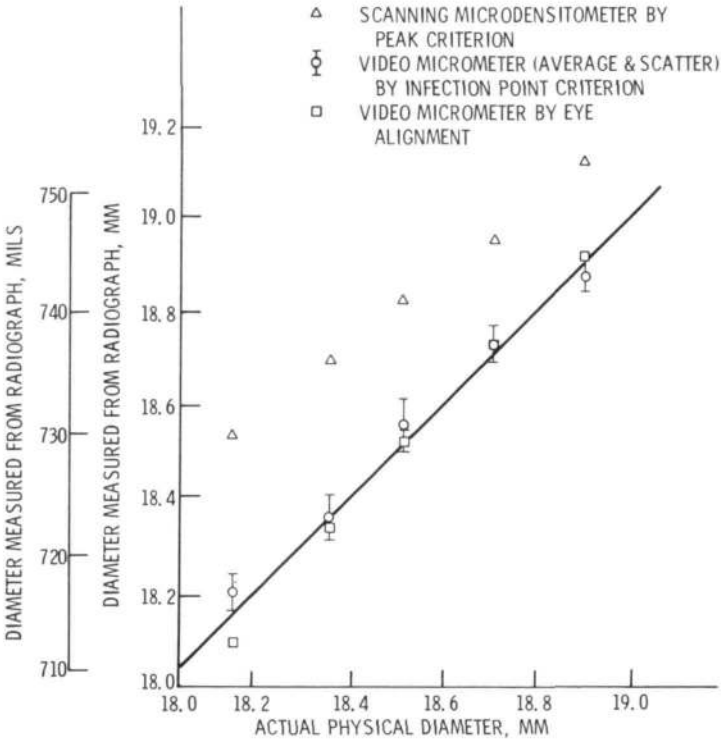

Figure 16. - Comparison of methods of measurement applied to radiographic test standard.

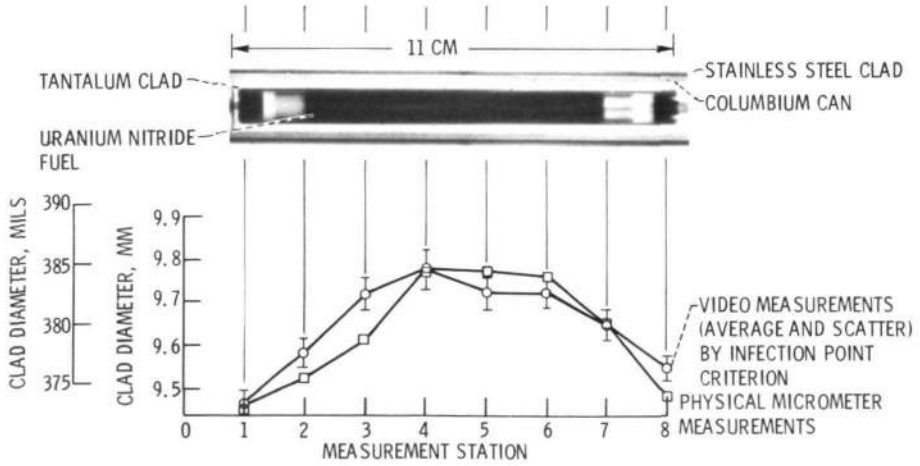

Figure 17. - Comparison of clad swelling measurements for an irradiated uranium nitride fuel element.